# Raman spectroscopy and AC conductivity of polyaniline montmorillonite (PANI–MMT) nanocomposites

**Abdul Shakoor · Tasneem Zahra Rizvi · Ahmad Nawaz**

**Abstract** A series of polyaniline/montmorillonite clay (PANI–MMT) nanocomposites were synthesised by in situ polymerisation of aniline in acidic medium in the presence of varying amounts (from 1 to 30 wt%) of MMT and a substoichiometric amount of ammonium persulfate (APS). For a preferred molar ratio of monomer to oxidant of 2:1, the aniline was polymerised and largely incorporated into the MMT. The PANI–MMT nanocomposites were characterised and compared by wide-angle powder X-ray diffraction and UV–Vis spectroscopy. Raman spectroscopy was used to investigate the interaction between clay layers and the intercalated polymer chains. Room temperature AC conductivity was measured in the frequency range 30 Hz to 1 MHz. Pure PANI and all the composites exhibited a low frequency region of frequency independent AC conductivity followed by a high frequency dispersive region where the AC conductivity obeyed a fractional power law of frequency dependence. The fractional exponent **n** for all the nanocomposites is significantly high as compared to that of pure PANI; **n** = 0.9 for all the composites whereas for pure PANI **n** = 0.2. In pristine PANI the onset of the dispersive region $\omega_c$ is at a much higher frequency (at 300 kHz) as compared to the nanocomposites in which $\omega_c$ is about 10 kHz.

## 1 Introduction

Among the conducting polymers, special interest has been focused on PANI due to excellent thermal and environment stability combined with relatively high level of electrical conductivity. Nevertheless a few applications have been reported based on PANI because it exhibit poor mechanical properties.

For the commercial use of conducting polymer composites, a complete understanding of their properties is necessary. Considerable efforts have been made over several decades to study the effect of filler on the dynamic electric and mechanical properties of the polymers [1, 2]. Also a number of attempts have been made to provide a theoretical description of the conducting mechanism [3] in the presence of grains embedded in the polymers. Polymer-MMT intercalation compounds (nanocomposites) have been investigated by a number of researchers. Owing to its use of natural clay materials and a water-based polymerisation system, the PANI–MMT system [4–19] addresses concerns on environmental and health issues. MMT has a very low toxicity, a low cost and a galleried structure, making it a very good host material. Despite a large number of studies on PANI–MMT system intercalated conducting polymer in host material like MMT is poorly understood. Although aniline can be polymerised by other techniques [11], including emulsion polymerization [13–16] and solvent-free mechano-chemical polymerisation [20–23], we chose a suspension method already reported in the literature [24] because it is a very easy procedure and generally produces homogeneous polymers. As regards charge transport process in conducting polymers there have been many studies that investigate DC conductivity as a function of temperature and/or doping level in different types of conducting polymers including

A. Shakoor (✉)
Physics Department, B.Z. University, Multan, Pakistan
e-mail: khan_9547@hotmail.com

T. Z. Rizvi · A. Nawaz
Physics Department, Quaid-I-Azam University, P.O. Box 45320, Islamabad, Pakistan

conjugated organic polymers, the inorganic polymer polysulphur nitride, alkali-metal fulleride polymers, and carbon nanotubes and have been reviewed and compared [17, 18]. Review of the literature, however, reveals that AC conductivity studies of Polyaniline intercalated into the layers of montmorillonite (MMT) clay are scarce [16, 20]. Here in this paper we investigate the effect of MMT concentration on AC conductivity of PANI–MMT nanocomposites. Raman spectroscopy is employed here to study the systematic change in subtle interactions between MMT and intercalated PANI on increasing the MMT content in the nanocomposites.

## 2 Experimental

Aniline (99%) was obtained from Sigma–Aldrich and was vacuum-distilled before use. Ammonium persulfate (APS) was obtained from Fluka and montmorillonite (MMT) powder was supplied by Sigma–Aldrich and was used as received. PANI–MMT composites were synthesized by a suspension method in which MMT was loaded from 0% to 30% in aniline in the presence of HCl and was polymerised by dropwise addition of APS solution. This synthesis method has already been reported in the literature [24].

Pressed pellets for conductivity studies were prepared in a stainless steel die of 13 mm diameter and 1 mm thickness using KBr press machine under 10 ton pressure. DC conductivity was measured by four probe method using Keithley 117 electrometers and a current source electrometer. AC conductivity was measured by using Wayne Kerr LCR meter Model 4275 in the frequency range 100 Hz to 1 M Hz.

X-Rays powder diffraction analysis was carried out using an automated diffractometer, Bruker-AXS model D8, using Cu–K$_\alpha$ radiations. The instrument was operated at 40 kV and 30 mA and diffraction patterns of PANI–MMT samples mounted on a standard holder were recorded over the range of 3°–40° counting time was 3 s and the step size was 0.1°. Raman spectra for 633 nm exciting radiation were recorded on a Renishaw RM 1000 laser Raman (He–Ne ion) containing an Olympus metallurgical microscope and a CCD detector. The laser power at the sample was kept below ∼0.74 mW to avoid thermal degradation. The laser was focused using a 50× objective lens and spatial resolution was about 1 μm. UV–visible absorption spectra of all the PANI–MMT composites were recorded on a Varian CARY 100 double-beam scanning spectrophotometer. The PANI–MMT composites dispersed in chloroform were spin-coated onto quartz glass substrates, and spectra were recorded from 200 to 800 nm wavelength.

## 3 Results and discussions

Figure 1 compares the powder XRD patterns of PANI–MMT composites. The broad, amorphous peak (18–22°) in pure PANI (Fig. 1a) was found in all the PANI–MMT composites and confirmed that polyaniline was present in all composites according to its expected proportion. A small, diffuse peak at 5.5° in MMT clay was at the same position in all the PANI–MMT composites but was absent from the pattern for pure PANI (Fig. 1a). The strong, sharper peak at 8.9° was also present in all the PANI–MMT composites (Fig. 1d, e). The intensity of this peak increased with the proportion of MMT. A sharp peak at 26.9° due to SiO$_2$ in MMT was observed to be unchanged in all the PANI–MMT composites (Fig. 1b–e).

The interlayer spacing increased from 1.64 nm in pure MMT to 1.92 ± 0.01 nm for 1–5% MMT, as a result of the intercalation and polymerisation of anilinium ions. The magnitude of this expansion indicates that the aniline rings lie parallel to the inorganic planes. The insulating silicate layers weaken the electronic interactions between the PANI chains and depress the interchain conductivity. In the 1, 5 and 10% MMT composites, these silicate layers incorporate PANI, but many chains are expected to interlink the MMT crystallites; therefore in these composites the conductivity is still reasonably high, whereas for 20 and 30% MMT the silicate layers increasingly isolate the conductive PANI chains (Table 1). XRD, temperature dependant DC conductitity along with FT-IR, SEM and TGA are explained in detail in the literature [24].

## 4 AC conductivity of PANI–MMT

The DC and AC transport are both due to the same mechanism. A proper understanding of the AC
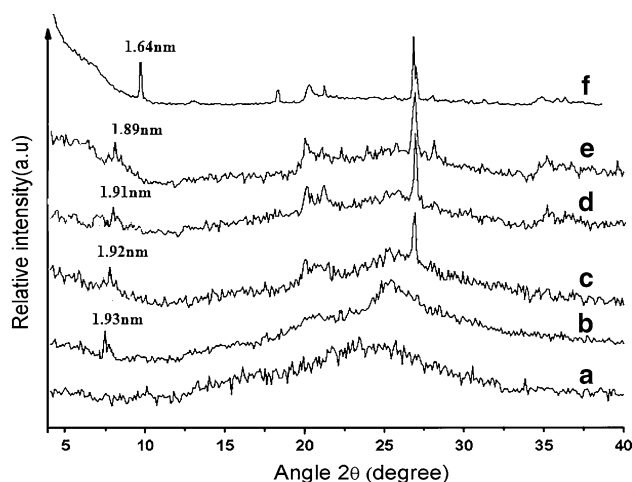


**Fig. 1** X-Ray diffraction of **a** PANI, **b** 1% MMT, **c** 10% MMT, **d** 20% MMT, **e** 30% MMT and **f** MMT

**Table 1** Variation of d-spacing, and conductivity as a function of MMT loading in PANI

| Sample | Interlayer d-spacing (nm) | DC conductivity $(S.cm^{-1})$ | AC conductivity (S/cm) | |
|---|---|---|---|---|
| | | | At 100 Hz | At $10^6$ Hz |
| MMT | 1.64 | – | | |
| PANI | | 0.47 | 0.58 | 1.25 |
| 1% MMT in PANI | 1.93 | 0.43 | 0.51 | 3.16 |
| 5% MMT in PANI | 1.91 | 0.167 | 0.40 | 3.64 |
| 10% MMT in PANI | 1.92 | 0.137 | 0.31 | 4.13 |
| 20% MMT in PANI | 1.90 | 0.078 | 0.13 | 4.78 |

conductivity is necessary to have a complete picture of the DC transport [25]. By hopping backward and forward at places with high jump probability a charge carrier may significantly contribute to the AC conductivity, while the DC conductivity is determined by the overcoming of unfavorable places in the solid for the formation of a continuous 'percolation' path between the electrodes.

Measured AC conductivity values in pure PANI and all its MMT composites are shown as a function of frequency in Fig. 2. Pure PANI and all the composites exhibit a low frequency region of frequency independent AC conductivity followed by a high frequency dispersive region where the AC conductivity follows a fractional power law of frequency dependence. The general behaviour of low frequency region of frequency independent AC conductivity and high frequency dispersive region has also been observed in a recent study of mechano-chemically synthesized PAN–MMT nanocomposites [20] at all temperatures in the range 23–200°C. Our results, however, can not be compared quantitatively with the referred study because it involved different reactants, different synthesis procedure and different aniline to oxidant ratios.
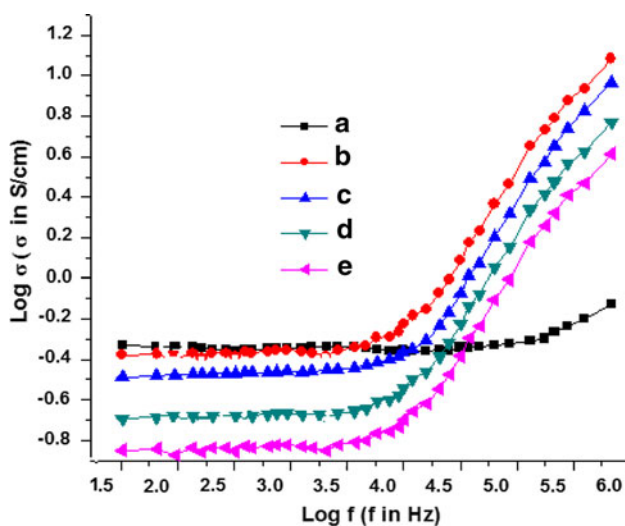


**Fig. 2** AC conductivity of **a** PANI, **b** 1% MMT, **c** 5% MMT, **d** 10% MMT and **e** 20% MMT in PANI

The real part of the electrical conductivity $\sigma(\omega)$ can be expressed as:

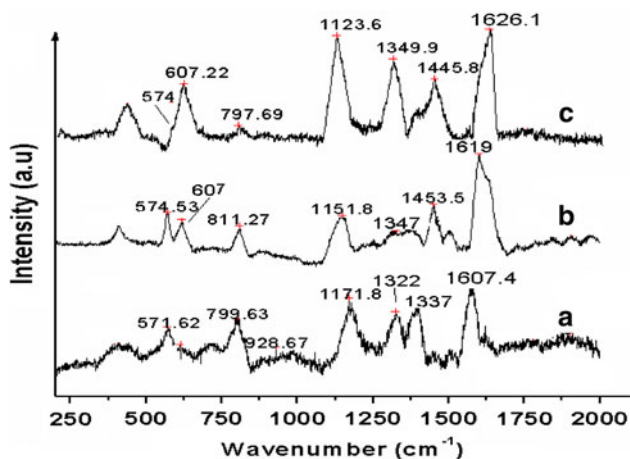$$\sigma(\omega) = \sigma_0 + A\omega^n \tag{1}$$

where $\sigma_0$ denotes the DC conductivity, "A" the constant, $\omega$ the angular frequency of the applied field and $n \leq 1$ is a fractional exponent. As is evident from Fig. 2, the fractional exponent $n$ for all the nanocomposites is significantly high as compared to that of pure PANI ($n = 0.9$ for all the composites whereas for pure PANI $n = 0.2$). It may further be noted that in pristine PANI the onset of the dispersive region $\omega_c$ is at a much higher frequency (at about 300 kHz) as compared to the nanocomposites in which $\omega_c = 10$ kHz.

The fractional power dependence of the AC conductivity upon frequency has been observed in a wide variety of disordered materials, such as amorphous semiconductors, polymers and ionically conducting glasses [26]. It has been suggested that the power law of Eq. (1) originates from many-body interactions between the hopping charges [26]. Equation (1) is widely used to describe AC conductivity in conducting polymers [27–29]. In disordered systems, where hopping transport occurs, the AC conductivity increases as the frequency of the applied electric field increases, because of the contribution of charge carriers moving along shorter and shorter distances, i.e., confined inside smaller and smaller clusters. In this sense, the fractional exponent expresses the relative reduction of clusters upon frequency. Exponents close to unity are associated with 'lattice' response, while values smaller that unity are related with the presence of impurities or injected carriers [30]. Therefore, the fractional dispersion of the AC conductivity may provide a useful diagnostic tool for characterizing charge transport in such materials [31].

It is an experimental fact that the measured conductivity $\sigma_{AC}(\omega)$ consists of two components: One results from charge transfer along the paths extending along the volume of the specimen, which contribute to the macroscopic $\sigma_{DC}$ and the second component results from the charge flow along paths of length $L_k$ equal to or longer than a critical length $L_c = v/\omega_c$ [32]. A significantly high value of $\omega_c$ in pure PAni as compared to all its clay composites depicts a

smaller critical length $L_c$ in pure PAni as compared to its clay composites which can be explained in terms of smaller average cluster size in pure PAni as compared to its MMT composites. Intercalation of PAni inside the clay galleries results in an increase in the average cluster size due to straightening and linearizatioon of polymer chains which gives rise to an overall increase in structural order in the polymer.

Raman spectroscopy used in the microscope mode is very efficient for the characterization of interactions between the components in polymer composites and blends [33] Raman spectra using laser line at 632.8 nm exciting radiation was recorded. Figure 3 compares the Raman spectra of PANI–MMT with different proportion of MMT. It is possible to observe intense overlapping bands at 1,322 and 1,337 $cm^{-1}$, corresponding to C–N$^+$, stretching modes of delocalized polaronic charge carriers, which is characteristic of the protonated imine form of polyaniline. The band at 1,322 $cm^{-1}$ is shifted to 1,347 and 1,349 $cm^{-1}$ with 10 and 20% MMT and the band at 1,337 $cm^{-1}$ is shifted to 1,453 and 1,445 $cm^{-1}$ with 10 and 20% MMT respectively. Moreover two important absorptions can be highlighted: at 607 $cm^{-1}$, related to benzene ring deformation [33] and at 571 $cm^{-1}$, assigned to crosslinking between PANI chains [34] The band at 607 $cm^{-1}$ has been attributed to the deformation of the benzene ring in the PANI backbone, and according to the literature [35] it may be enhanced by the presence of other insulating materials, Therefore, the presence of the band at 607 $cm^{-1}$ in composites containing 10 and 20% MMT in PANI Fig. 3b, c imparts good interaction between the MMT matrix and the polyaniline propagating. As the amount of insulating materials is enhanced the band at 571 $cm^{-1}$ is shifted at 574 $cm^{-1}$ and its intensity decrease for nanocomposite with 20% MMT. When the MMT content in the nanocomposites exceeds 10% the insulating behaviour of MMT clay becomes more prominent as indicated by vanishing of the band at 574 $cm^{-1}$ and enhancement of the band at 607 $cm^{-1}$ in the nanocomposite with 20% or higher MMT contents.

The bands at 1,171 and 1,607 $cm^{-1}$, assigned to C–H, and C–C of benzenoid units, respectively are observed in PANI spectrum [36]. The same bands are observed for all PANI–MMT composites with a little shift. One important point is the non-observation of other bands in those PANI–MMT composite spectra that could be assigned to other chromophores present in polymeric chains. New bands have been observed in the spectrum of PANI–MMT along with PANI bands and some bands have shifted as well which is an evidence of some formation of some new bonds due to intercalation of PANI in MMT layers as has been observed in UV and XRD data. Moreover it can be infered from Raman spectra that the composites with 10% MMT has maximum interaction with conducting polymer due to which the conductivity is reasonable high (of the same order of magnitude as of pure PANI) as compared to that of 20% and higher amount of MMT in PANI–MMT composites.

The UV–Vis spectra of all nanocomposites in this study are shown in Fig. 4. Two major characteristics peaks can be observed at about 380 and 670 nm wavelengths. The absorption at 380 nm is due to polaron-$\pi^*$ transition and the second band at 670 nm can be assigned to exciton transition between benzenoid and quinoid rings [37, 38]. The second band at 670 nm is slightly shifted to lower wavelength which indicated the interaction between PANI and MMT. The intensity of 670 nm band decreases with the increase in MMT loading which shows the deformation in benzenoid ring which has also been observed in Raman spectra. The composite with 5 and 10% MMT has prominent intensity of this band but the composites with 20 and 30% MMT have very low intensity at this wavelength.



**Fig. 3** Raman spectra of **a** PANI, **b** 10%, **c** 20% MMT in PANI
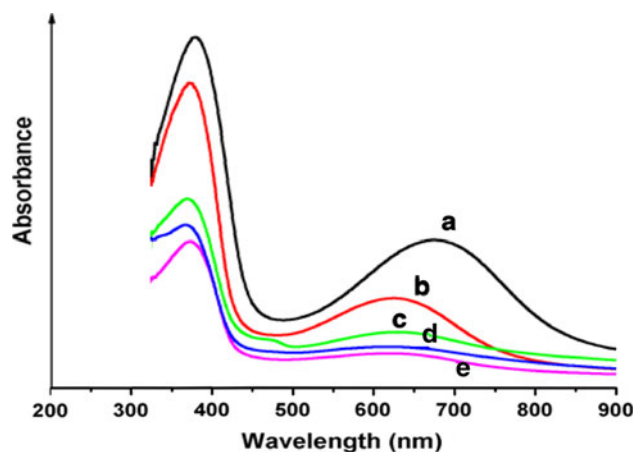


**Fig. 4** UV–Vis spectroscopy of **a** PANI, **b** 5% MMT, **c** 10% MMT, **d** 20% MMT and **e** 30% MMT in PANI

Therefore, we can say that as regards the conductivity values the composites with 5 and 10% MMT are far better than 20 and 30% MMT composites.

## 5 Conclusion

Plyaniline/montmorillonite clay (PANI–MMT) composites have been synthesised by solution polymerisation in the presence of hydrochloric acid and a substoichiometric amount of ammonium persulfate (APS), with molar ratio of monomer to oxidant of 2:1, the aniline was polymerised and largely incorporated into the MMT, which was confirmed by XRD, Raman spectra and UV–Vis spectroscopy shows some peaks shifts, which indicate the formation of some new bonds and support the intercalation of PANI chains into the interlayer spacing of Montmorillonite MMT clay. The interaction of PANI and MMT has been observed to be maximum for the composite with 1% MMT and is found to decreases slowly with the subsequent addition of MMT in the nanocompsites. Both DC and low frequency AC conductvities are found to decrease with the MMT contents in the nanocomposites exhibiting the insulating character of MMT in the composites. AC conductivities of the nanocompsites at high frequencies, however, are found to be signifintly high as compared to pure PANI which indicates higher backward and forward jump probabilities of the charge carriers in the nanocomposites as compared to the pristine PANI at high frequencies and hence making these nanocomposites a better choice for high frequency conductivity applications.

## References

1. S.T. Lim, Y.H. Hyun, H.J. Choi, M.S. Jhon, Chem. Mater. **14**, 1839–1844 (2002)
2. Z. Ding, J.T. Kloprogge, R.L. Frost, G.Q. Lu, H.Y. Zhu, J. Porous. Mater. **8**, 273–293 (2001)
3. A.K. Jonscher, Nature (Lond.) **267**, 673 (1977)
4. B.H. Kim, J.H. Jung, S.H. Hong, J. Joo, Macromolecules **35**, 1419 (2002)
5. B.H. Kim, J.H. Hong, J.W. Kim, H.J. Choi, J. Joo, Curr. Appl. Phys. **1**, 115 (2001)
6. D.C. Lee, L.W. Jang, J. Appl. Polym. Sci. **61**, 1117 (1996)
7. G.M. do Nascimento, V.R.L. Constantino, R. Landers, M.L.A. Temperini, Macromolecules **37**, 9373–9385 (2004)
8. G.M. do Nascimento, V.R.L. Constantino, R. Landers, M.L.A. Temperini, Polymer **47**, 6131–6139 (2006)
9. G.M. do Nascimento, M.L.A. Temperini, Eur. Polym. J. **44**, 3501–3511 (2008)
10. G.M. do Nascimento, C.H.B. Silva, C.M.S. Izumi, M.L.A. Temperini, Spectrochimica Acta Part A **71**, 869–875 (2008)
11. F.F. Fei, J.C. Hyoung, J. Jinsoo, J. Nanosci. Nanotechnol. **8**, 1559–1581 (2008)
12. Q.Y. Soundararajah, B.S.B. Karunaratne, R.M.G. Rajapakse, Mater. Chem. Phys. **113**, 850–855 (2009)
13. V.L. Reena, J.D. Sudha, C. Pavithran, J. Appli. Polym. Sci. **113**, 4066–4076 (2009)
14. D.H. Song, H.M. Lee, H.J. Choi, J. Nanosci. Nanotechnol. **9**, 1501–1504 (2009)
15. F. Sun, Y. Pan, J. Wang, Z. Wang, C. Hu, Q. Dong, Polym. Compos. **31**, 163–172 (2010)
16. D.M.M. Krishantha, R.M.G. Rajapakse, D.T.B. Tennakoon, H.V.R. Dias, Ionics **12**, 287–294 (2006)
17. A.B. Kaiser, Rep. Prog. Phys. **64**, 1 (2001)
18. A.B. Kaiser, Adv. Mater. **13**, 927–941 (2001)
19. N. Boutaleb, A. Benyoucef, H.J. Salavagione, M. Belbachir, E. Morallón, Eur. Polym. J. **42**, 733–739 (2006)
20. I. Bekri-Abbes, E. Srasra, React. Funct. Polym. **70**, 11–18 (2010)
21. A. Shakoor, T. Z. Rizvi, Poly. Sci. Ser. A Polym. Phys. **52**, 55–59 (2010)
22. S. Yoshimoto, F. Ohashi, T. Kameyama, Polym. Phys. **43**, 2705–2714 (2005)
23. S. Yoshimoto, F. Ohashi, T. Kameyama, Macromol. Rapid Commun. **25**, 1687–1690 (2004)
24. A. Shakoor, P.J.S. Foot, T.Z. Rizvi, J. Polym. Polym. Comp. **17**, 347–352 (2009)
25. J. Dyre, J. Appl. Phys. **64**, 2456 (1988)
26. A.K. Jonscher, *Dielectric relaxation in solids* (Chelsea Dielectrics Press, London, 1983)
27. E. Singh, A.K. Narula, R.P. Tandon, A. Mansingh, S. Chandra, J. Appl. Phys. **80**, 985 (1996)
28. P. Dutta, S. Boswas, K.D. De, J. Phys. **13**, 9187 (2001)
29. K. Jager, H. Mcqueen, M. Techmutin, M. Kluppel, J. Phys. D **34**, 2699 (2001)
30. S. Capaccioli, M. Lucchesi, P.A. Rolla, C. Ruggeri, J. Phys. **10**, 5595 (1998)
31. A.K. Jonscher, Nature **267**, 673 (1977)
32. A.N. Papathanassiou, I. Sakellis, J. Grammatikakis, Appl. Phys. Lett. **91**, 122911 (2007)
33. M. Cochet, G. Louarn, S. Quillard, J.P. Buisson, S. Lefrant, J. Raman Spectrosc. **31**, 1041 (2000)
34. M. Tagowska, B. Palys, K. Jackowska, Synth. Met. **142**, 223 (2004)
35. G. Louarn, M. Lapkowski, S. Quillard, A. Pron, J.P. Buisson, S. Lefrant, J. Phys. Chem. **100**, 6998 (1996)
36. J.E. Pereira da Silva, D.L.A. Faria, S.I.C. Torresi, M.L.A. Temperini, Macromolecules **33**, 3077 (2000)
37. Y.H. Kim, C. Foster, J.C. Chiang, A.J. Heeger, Synth. Met. **29**, 285–290 (1989)
38. F.L. Lu, F. Wudll, M. Nowak, A.J. Heeger, J. Am. Chem. Soc. **108**, 8311–8313 (1986)